

Surface x-ray diffraction on K/Si(001)(2×1) and Cs/Si(001)(2×1)

H. L. Meyerheim

Institut für Kristallographie und Angewandte Mineralogie, LMU München, D-80333 München, Germany

N. Jedrecy and M. Sauvage-Simkin

LURE, CNRS-MENRT-CEA, Bâtiment 209d, Centre Universitaire, F-91405 Orsay, France

and Laboratoire de Minéralogie-Cristallographie, Associé au CNRS et aux Universités Pierre et Marie Curie (Paris 6) at Denis Diderot (Paris 7), 4 place Jussieu, F-75252 Paris Cedex 05, France

R. Pinchaux

LURE, CNRS-MENRT-CEA, Bâtiment 209d, Centre Universitaire, F-91405 Orsay, France

and Université Pierre et Marie Curie, 4 place Jussieu, F-75252 Paris Cedex 05, France

(Received 2 February 1998)

The geometric structures of K/Si(001)(2×1) and Cs/Si(001)(2×1) formed at room temperature have been investigated using surface x-ray diffraction. The analysis of the intensity distribution along both half-order and integer-order reciprocal-lattice rods (135 and 113 independent reflections in total for K and Cs, respectively) indicates that at saturation coverage in both cases the alkali metal (*A*) adsorbs in two different sites. The average adsorption sites on the clean Si surface are at the dimer bridge site on top of the dimer rows, and at the valley bridge site in the groove between the Si dimers. Actually, the dimerization is (at least partially) lifted upon *A* adsorption. There is no evidence for a large *z* disorder of the top-layer Si atoms, which would be characteristic of an asymmetry of the Si-Si dimer. We derive K-Si bonding lengths in the range between 2.90 and 3.58 Å, and Cs-Si bonding lengths between 3.33 and 3.50 Å. The minimum bond lengths are at most 11% lower than values found in bulk KSi and CsSi. This can be interpreted by the formation of a weak covalent bond. In order to obtain good fits to the data, up to four layers of the Si substrate have to be included into the refinement. The Si-Si distances do not deviate by more than 5–10% from the bulk Si-Si bond length (2.35 Å). The only significant difference between the K and Cs adsorption structures is found for the alkali saturation coverage. For K we find a coverage of 1.2 ML, whereas only 0.3 ML is found for Cs.

[S0163-1829(98)05527-1]

I. INTRODUCTION

The adsorption of alkali metals (*A*'s) on Si(001)(2×1) is one prominent subject in surface science.^{1–3} It serves as a prototype to study the chemisorption and metallization of a semiconductor surface. One of the most important features of *A* adsorption is the lowering of the substrate work function and the promotion of surface chemical reactions such as the oxidation of Si.^{4,5} Despite the simplicity of the *A* electronic structures, and the detailed knowledge of the (2×1)-reconstructed Si(001) surface, there is still considerable controversy about many details of the *A*/Si(001)(2×1) adsorption geometry as well as about the electronic structure. Figure 1(a) shows, in top view, the (2×1)-reconstructed Si(001) surface. Large and small open circles represent first-layer dimer atoms and second-layer Si atoms labeled by Si₍₁₎ and Si₍₂₎, respectively. The (2×1) unit cell is indicated by the dashed rectangle, where the *a* and *b* axes of the unit cell are parallel to the [110] and [110] directions of the bulk Si lattice.⁶ The capital letters label high-symmetry alkali adsorption sites, namely, *P* (pedestal), *D* (dimer bridge), *T* (top), *T3* (top third Si layer), and *T4* (top fourth Si layer). The latter are also commonly referred to as valley bridge (*T3*) and cave site (*T4*) in the literature. Almost all these sites, as well as combinations of them, have been suggested on the basis of a wide spectrum of surface science techniques. Considerable controversy about the re-

sults still exists. In our previous investigation of the alkali adsorption on Ge(001)(2×1),⁷ we gave an overview; therefore we discuss here only some important results published so far.

In 1973, Levine⁸ suggested the *P* site for Cs/Si(001)(2×1) corresponding to a metallic overlayer and a saturation coverage of 0.5 ML. 1 ML corresponds to two alkali atoms per (2×1) unit cell, which means a coverage of 6.78×10^{14} atoms/cm². On the basis of angular-resolved ultraviolet photoelectron spectroscopy (ARUPS) data, Enta *et al.* concluded the K/Si(001)(2×1) surface to be semiconducting.⁹ In this context according to x-ray photoelectron diffraction data, Abukawa and Kono¹⁰ proposed the “double-layer model” for K and Cs with simultaneous adsorption of the alkali atoms in *T3* and *P* and a saturation coverage of 1 ML. This structure model has found considerable support through experimental as well as theoretical investigations.^{11–17} However, studies using low-energy electron-diffraction (LEED) by Urano and co-workers^{18,19} could not unambiguously discriminate between single- and double-layer models for K and Cs. The nature of the *A*-Si bond also is controversial. A mainly ionic bond for K on Si(001)(2×1) and a saturation coverage of 1 ML was proposed by Batra,²⁰ but other authors favored the picture of a (weak) polarized covalent bond and a metallic surface.^{21,22} The most recent high-resolution core-level spectroscopy and ARUPS experiments on K and Cs on Si(001) (Refs. 23–25)

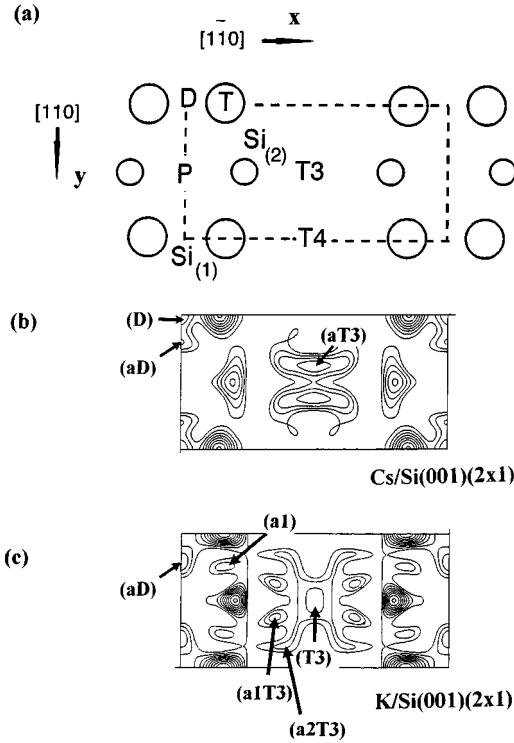


FIG. 1. (a) Schematic view of the (2×1) -reconstructed Si(001) surface projected along $[001]$. Large and small open circles labeled by $\text{Si}_{(1)}$ and $\text{Si}_{(2)}$ represent top- and second-layer Si atoms, respectively. The (2×1) unit cell is shown dashed. High-symmetry adsorption sites are indicated by D (dimer bridge), P (pedestal), T (top), $T3$ (top third layer), and $T4$ (top fourth layer). (b) Z -projected electron-density contour plot calculated on the basis of the $|F_{hk0}|$ for $\text{Cs/Si}(001)(2 \times 1)$. Apart from the maxima related to $\text{Si}_{(1)}$ and $\text{Si}_{(2)}$ additional Cs-related maxima can be identified. These are labeled by D , aD , and $aT3$, where the prefix “ a ” indicates an asymmetric site in the vicinity of the high-symmetric site. (c) Electron-density contour plot for $\text{K/Si}(001)(2 \times 1)$ as in (b).

suggested two different A adsorption sites and a metallic surface at saturation coverage. Moreover, the saturation coverage is also under controversy. Whereas Asensio *et al.*⁵ as well as Soukiassian *et al.*²⁶ proposed a saturation coverage of only 0.5 ML for K, the authors of Refs. 27, 28, and 13 determined a saturation coverage of 1 ML. The latter authors also found a 1-ML saturation coverage for Cs on $\text{Si}(001)(2 \times 1)$.

Most surface structural analytical tools applied so far to the $A/\text{Si}(001)-(2 \times 1)$ interfaces rely on a delicate interpretation of the measured data. On the other hand, surface x-ray-diffraction (SXRD) intensities can be analyzed on the basis of the single scattering theory.²⁹ However, the SXRD technique demands a high surface long-range order. In our previous investigation of the $A/\text{Ge}(001)(2 \times 1)$ system,^{7,30} we showed that Na, K, and Cs adsorb at $T3$ and at an off-centered $T4$ position, with a saturation coverage in the 0.6–0.7-ML range in all cases. Although the bulk structures of ASi and AGe ($A = \text{K, Rb, Cs}$) are isotopic^{31–34} and a very similar behavior of the systems $\text{Cs/Si}(001)(2 \times 1)$ and $\text{Cs/Ge}(001)(2 \times 1)$ has been observed using x-ray photoelectron spectroscopy,³⁵ the surface geometric structures of the $A/\text{Si}(001)(2 \times 1)$ phases might be different from those on

$\text{Ge}(001)(2 \times 1)$. In this paper we will show that this is indeed the case. In the following sections the experimental details and the results will be discussed in detail.

II. EXPERIMENT

The experiments were performed using a six-circle UHV diffractometer at the superconducting wiggler beamline DW12 of the storage ring at LURE (Orsay, France). Prior to transferring the n -doped $\text{Si}(001)$ samples (size $12 \times 12 \times 3 \text{ mm}^3$) into the UHV chamber, they were cleaned by the Shiraki chemical etch method.³⁶ In UHV the sample was slowly annealed up to about 900°C to remove the oxide layer. After cooling down, a sharp two domain (2×1) LEED pattern could be observed. The high surface quality was also attested by the SXRD measurements. We used focused radiation at a wavelength of 0.887 \AA while always keeping the sample under total reflection conditions. Integrated intensities were collected by an energy dispersive detector by rotating the sample around its surface normal.²⁹ The full width at half maximum of the $(\frac{3}{2} 0 0)$ superlattice reflection was measured equal to 0.045° , equivalent to $\Delta q = 1.93 \times 10^{-3} \text{ \AA}^{-1}$ (including the factor 2π), which corresponds to a terrace width of about 3000 \AA . Deposition of Cs and K was achieved by thoroughly degassed SAES dispensers, thereby keeping the pressure in the mid- 10^{-10} -mbar range. Simultaneously to A deposition, we monitored the $(\frac{3}{2} 0 0)$ superlattice reflection, which in the case of K and Cs saturated at an intensity level twice the value measured with the uncovered samples. It should be emphasized that in this paper this coverage is identified with “saturation coverage.”

For the three-dimensional analysis of the adsorbate structures, both superlattice and crystal truncation rods (CTR’s) were measured up to a normal momentum transfer $q_z = 2.6$ reciprocal lattice units (rlu), equivalent to 3.01 \AA^{-1} . The reproducibility of symmetry-equivalent in-plane structure factor intensities, $|F_{hk0}|^2$, was used to estimate the overall systematic errors. We determined average agreement factors for the $|F_{hk0}|^2$ values in the range between 11% and 8% (Ref. 29) for the different data sets [two data sets for $\text{K/Si}(001)(2 \times 1)$, one for $\text{Cs/Si}(001)(2 \times 1)$]. Table I lists the $|F_{hk0}|^2$ and their standard deviations (σ) derived by taking the quadratic sum over systematic and statistical errors.²⁹ The reflection indices are related to the (2×1) superlattice cell, and the intensities are normalized to the (300) reflection to allow comparison. It can be seen directly that the $\text{K/Si}(001)(2 \times 1)$ intensity data of the first data set are fairly well reproduced in the second one. It should be noted that all data sets are completely independent of one another, in that in each case a new sample, a new preparation, and a new sample alignment has been used. For the out-of-plane data, the reproducibility is not that excellent, but still in the range below 15–20% as derived from symmetry-equivalent rods.

III. RESULTS AND DISCUSSION

The three-dimensional analysis was performed by fitting the experimental data sets (fractional rods and integer order CTR’s) to structural models using the z -projected electron densities derived from the in-plane data, $|F_{hk0}|^2$, as starting

TABLE I. Comparison of observed and calculated in-plane ($hk0$) structure factor intensities for K/Si(001)(2×1) (sample Nos. 1 and 2) and Cs/Si(001)(2×1). The reflection indices are related to the (2×1) unit cell, and the intensities are normalized to the (300) reflection for better comparison. The $|F^{\text{cal}}|^2$ are calculated on the basis of the best fit models (see Tables II and III). For each reflection, σ represents its standard deviation. N is the number of measured in-plane reflections, and I is the number of symmetry independent reflections of the in-plane data set. $R_u(|F|^2)$ is the unweighted residuum of the fits.

hkl	K/Si(001)(2×1)						Cs/Si(001)(2×1)		
	Sample No. 1			Sample No. 2			$ F^{\text{obs}} ^2$	σ	$ F^{\text{cal}} ^2$
	$ F^{\text{obs}} ^2$	σ	$ F^{\text{cal}} ^2$	$ F^{\text{obs}} ^2$	σ	$ F^{\text{cal}} ^2$			
100	23.31	2.79	23.52	24.96	2.34	25.80	1.82	0.78	3.63
110	65.08	7.66	65.37	63.65	5.95	64.37	110.22	9.04	110.20
300	100.00	11.76	99.67	100.00	9.33	99.04	100.00	8.26	101.06
310	0.97	0.41	3.21	1.36	0.65	2.54	1.24	1.33	0.54
120	18.80	2.28	16.07	16.72	1.63	13.10	24.10	3.33	20.21
320	108.76	12.81	109.21	108.09	10.13	107.71	61.56	5.29	57.76
500	94.98	11.20	95.57	72.94	6.84	71.69	58.03	6.04	59.62
510	3.86	0.62	6.36	2.41	0.67	6.06	7.45	2.16	3.37
520	5.40	0.92	6.86	2.88	0.72	1.12			
130	3.07	0.66	4.93	2.41	0.51	2.49	3.79	2.36	11.02
330				3.81	0.89	6.30	4.63	4.60	3.71
530	8.37	1.22	11.15	6.66	1.15	10.16			
700	6.72	0.92	6.34	3.69	0.71	3.37	2.45	2.94	1.88
710	19.34	2.36	17.04	18.35	1.90	15.87	29.23	4.80	24.70
720	8.93	1.30	7.82	12.15	1.67	5.84	2.71	2.87	9.19
730	2.28	2.60	3.91	1.80	1.80	2.95			
140	30.31	3.73	27.63	27.69	2.97	28.52	26.52	7.21	29.33
340	49.99	6.05	50.28	51.97	5.12	50.58			
540	10.60	2.92	7.57	5.17	1.75	5.01			
740				2.09	2.10	1.50			
900	2.61	1.67	1.39	6.00	6.03	1.84			
910				3.02	3.03	3.73			
N		54			48			31	
I		19			22			14	
$R_u(F ^2)$		4.98%			7.82%			9.09%	

models. These were derived from the calculation of the Patterson function and from difference Fourier syntheses in the same way as discussed in our previous work on A/Ge(001)(2×1).⁷ Figures 1(b) and 1(c) show the z projected electron densities $\rho(x,y)$ of the Cs/Si and K/Si interface at saturation coverage calculated on the basis of the best in-plane fit model using the corresponding calculated phases $\alpha_{hk0}^{\text{calc}}$.²⁹ The comparison with the clean Si(001)(2×1) structure model in Fig. 1(a) allows one to identify the electron density coming from Si₍₁₎ and Si₍₂₎, and the additional densities around the positions D and $T3$. Asymmetric sites are labeled by the prefix a . These structure models can be classified in the group “double-layer model,” but with the combination $D/T3$ instead of $P/T3$ as most frequently suggested in the literature.

Figure 2 compares some rods measured for Cs/Si(001)(2×1) and K/Si(001)(2×1). The measured structure factor amplitudes $|F|$ are represented by the symbols; the calculated amplitudes on the basis of the final model are shown by the solid lines. A direct comparison shows that some differences exist between the K and Cs adsorbate structures which are also evident from the in-plane

data. The overall agreement between measured and calculated $|F|$ for the three-dimensional data sets is reasonably good as expressed by the unweighted residua of $R_u = 10.9\%$ for Cs/Si(001)(2×1) and 8.9% for K/Si(001)(2×1).³⁷ In the final models for K/Si(001)(2×1) and Cs/Si(001)(2×1), we used 26 and 14 structural parameters (including the atomic displacement factors describing the disorder; see below), respectively, which are still in a reasonable proportion with respect to the number of measured reflections (134 and 113). The structure parameters are listed in Tables II and III. Figures 3 and 4 show schematically in top and side views the final structure models. The atoms are labeled according to Tables II and III; the A atoms are shown as hatched circles, where their relative size approximately corresponds to the A occupation factors. Significant disorder is emphasized by ellipses as shown for Si₍₁₎, and for some A 's. Several results can be summarized.

(1) In both systems the main A adsorption sites are at (or close to) the dimer bridge site D in Fig. 1(a) and at the site $T3$ above the third-layer Si atom in the center of the (2×1) unit cell. These basic structure models are directly evident from the inspection of the projected electron densi-

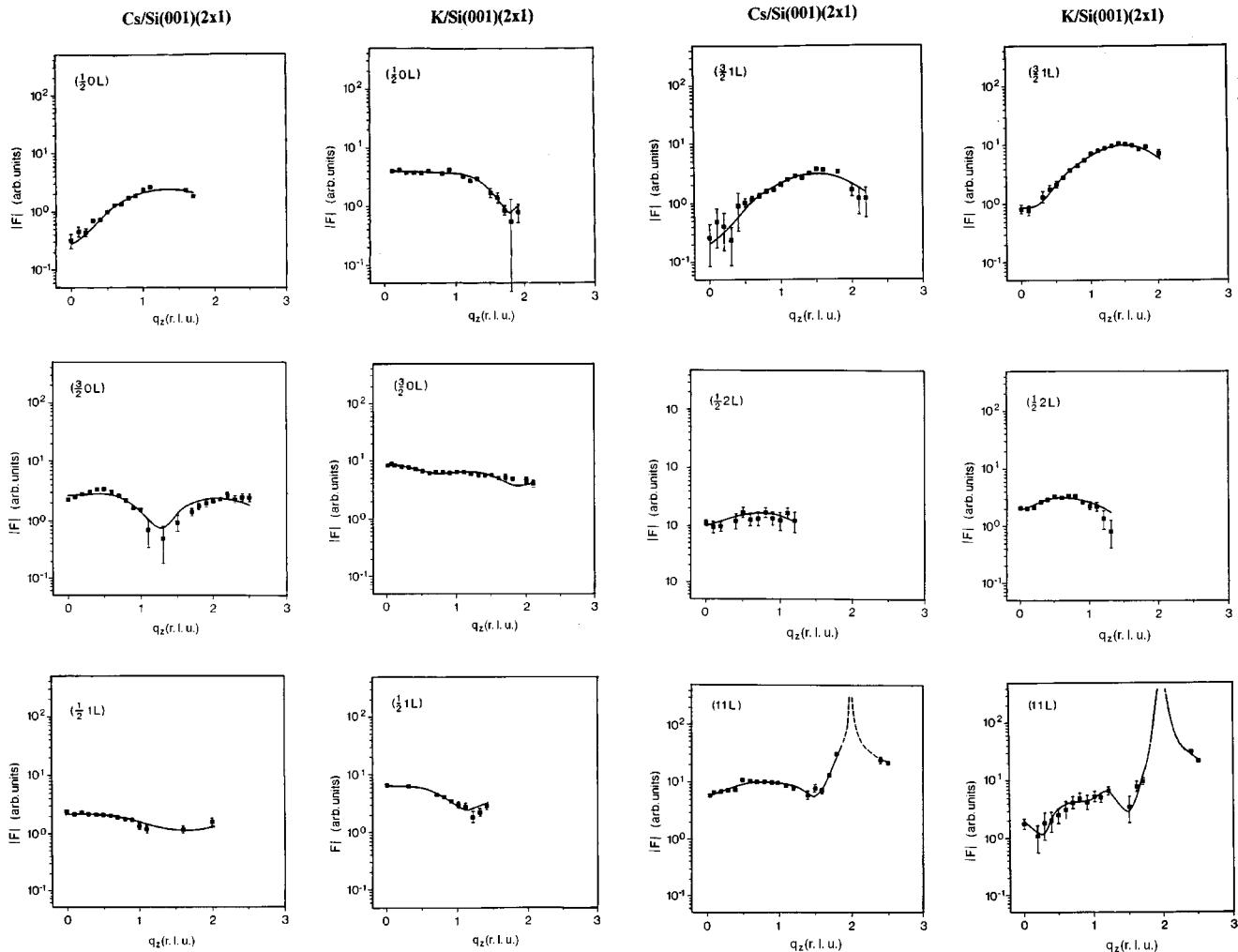


FIG. 2. Measured (symbols) and calculated (lines) structure factor amplitudes along several superlattice and crystal truncation rods for Cs/Si(001)(2×1) and K/Si(001)(2×1).

ties. However, in order to obtain good fits, it is necessary to introduce considerable disorder for the adatoms and the Si-substrate atoms. The disorder can be taken into account by (anisotropic) atomic displacement factors (ADP's) as well as by split positions. Without temperature-dependent measurements it is not possible to distinguish between dynamic and static disorder; therefore the term ADP is commonly used.³⁸ In the case of a K/Si(001)(2×1) system and *D*-site adsorption site it is the best choice to use a combination of the split position description and an anisotropic ADP. The asymmetric site is labeled by “*aD*.” For the *T3* site, the smearing out of the electron density visible in Fig. 1 can only adequately be modeled by low occupied additional sites (*a1T3*, *a2T3*) around *T3*. In the case of Cs/Si(001)(2×1) a combined description using split positions and ADP's is also necessary. The occupation of the off-centered sites *aT3* and *aD* is also directly evident from the projected structure shown in Fig. 1(b). We can summarize that the occupation of the sites *D*, *aD* and *T3*, *aT3* with large disorder is a common feature of both systems, except that the disorder is higher in the K case.

One important difference between K and Cs is that we observe an additional asymmetric K-adsorption site in the vicinity of the top-layer Si atoms, although with low occu-

pancy. This site is labeled by *a1*, and is also directly observable in the projected electron density in Fig. 1(c) as well as in the Patterson function (not shown). On first inspection this site appears to be quite unusual, in that it does not fit at all into the classical scheme of coordination maximization and high adsorption site symmetry. However, in the recent past “unusual” adsorption sites such as on-top or substitutional sites have been reported for *A*'s on low index metal surfaces.^{39,40} Theoretical calculations show that the occupation of these sites is a result of a delicate balance between different contributions to the total surface free energy.⁴¹ In the present case we may speculate that basically similar reasons might account for the K adsorption in the site *a1*, for example, interaction with the Si dangling bonds in the presence of additional K in the asymmetric sites around *T3*.

(2) The second main result is that the dimerization of the top layer Si atoms (*Si*₁) is (at least partially) lifted upon *A* adsorption. The positions of the *Si*₍₁₎ atoms along the *a* axis of the (2×1) unit cell are refined to 0.24(3) and 0.22(3) for Cs and K adsorption, respectively. This is close to the bulk position *x*=0.25. Moreover, there is no evidence of a significant *z* disorder which would be characteristic for asymmetric dimers such as determined in previous investigations on

TABLE II. Structure parameters for Cs/Si(001)(2×1) of the final model. Some distances in comparison with corresponding bond lengths in bulk structures are listed below. Lattice constants: $a_0=7.68$ Å, $b_0=3.84$ Å, and $c_0=5.43$ Å. Nonstructural parameters: two scale factors, roughness factor $\beta=0.156$. 113 reflections: $R_u=0.109$. Covalent Si-Si distance: 2.35 Å. Theoretical distances: Si-Cs⁰: 3.85 Å. Si-Cs⁺: 2.84 Å. Distances in bulk CsSi: Average distance 3.76 Å (minimum 3.56 Å) [see, e.g., E. Busmann, Z. Anorg. Allg. Chem. **313**, 91 (1961)]. * $B=8\pi^2U$, where U is the mean squared displacement amplitude.

Atom	x	y	z	ADP (Å ²)	Occupancy
Cs _(D)	0.00 ^a	0.00 ^a	-0.51(2)	$B=13(5)^*$	0.04(1)
Cs _(aD)	0.00 ^a	0.24(2)	-0.52(2)	$U^{11}=0.06(4)$ $U^{22}=0.08(4)$ $U^{33}=0.35(10)$	0.11(3)
Cs _(aT3)	0.50 ^a	0.25(2)	-0.49(2)	$U^{11}=0.10(3)$ $U^{22}=0.23(5)$ $U^{33}=0.40(10)$	0.14(3)
Si ₁	0.24(3)	0.00 ^a	0.00 ^a	$U^{11}=0.20(10)$ $U^{22}=0.01^a$ $U^{33}=0.01^a$	1.00 ^a
Si ₂	0.25(2)	0.41(2)	0.14(2)	$B=8(1)$	0.50 ^a
Si ₃₁	0.00 ^a	0.50 ^a	0.41(2)	$B=7(5)$	1.00 ^a
Si ₃₂	0.50 ^a	0.50 ^a	0.41(2)	$B=7(5)$	1.00 ^a
Interatomic distances (Å), error≈0.15–0.30 Å					
	Cs _(D) -Si ₁ :	3.33			
	Cs _(aD) -Si ₁ :	3.50			
	Cs _(aT3) -Si ₁ :	3.46			
	Cs _(aT3) -Si ₂ :	4.04 ^b			
	Si ₁ -Si ₂ :	2.07 ^b			
	Si ₂ -Si ₃₁ :	2.44 ^b			
	Si ₂ -Si ₃₂ :	2.44 ^b			

^aFixed parameter during refinement.

^bAverage distance over Si₍₂₎ split positions.

clean and alkali-covered Ge(001)(2×1).^{7,30,42} We may speculate that the relaxation of the Si dimerization is a consequence of the charge transfer from the adsorbed A's to the dangling bonds of the Si atoms. However, we observe considerable disorder of Si₍₁₎ along the a axis as expressed by mean-squared displacements (U^{11}) of 0.20 Å². On the basis of this result we tentatively assume that some fraction of symmetric dimers is still present, and that the large disorder is a result of the averaging over different configurations, namely, symmetric dimers and Si atoms close to their bulk positions. For example, in the case of a split position model for Si₍₁₎ which uses two Si positions along the a axis (each with occupancy 0.5 and fixed $B=0.6$ Å²) the refinement leads to x positions at 0.27(3) and 0.17(3), the latter corresponding to a Si-Si bond length of 2.61 Å. Although this value is significantly larger than the bulk Si-Si distance (2.35 Å) it is still in the range to allow the interpretation that the Si-Si dimer bond still exists.

Photoemission as well as structure investigations have shown the influence of charge transfer on the dimer structures.²¹ In particular this has been suggested for K/Si(001)(2×1) (Ref. 23) using XPS, but not for Cs/Si(001)(2×1).²⁴ In addition to the removal of the dimer asymmetry, Wei *et al.*⁴³ determined a Si-Si bond relaxation upon Na adsorption. In their LEED analysis, they proposed a model with Na adsorbed only in the P site, and a Si-Si dis-

tance of 2.64 Å. Our model is the presence of two configurations, a (weakly bonded) symmetric Si-Si dimer and a fully lifted Si dimerization, and might be related to the different and disordered A adsorption sites on the surface.

(3) The A -Si₍₁₎ bond lengths are found to be somewhat lower than the corresponding bond lengths in the bulk ASi structures.^{31–34} For Cs, we determine a minimum Cs-Si bond length of 3.33(25) Å from the D site to Si₍₁₎ which has to be compared with the minimum bond length in bulk CsSi (3.56 Å). The Cs-Si₍₁₎ distances from the sites aD and $aT3$ are 3.50(25) and 3.46(25) Å, respectively, i.e., in the range found in bulk CsSi. The Cs adsorption in the asymmetric position $aT3$ might be explained with the formation of a covalent Cs-Si bond with the optimum length. This is because a Cs-Si bond distance in the regime of 3.50 Å with a Cs in $T3$ could only be realized with a lower z value above the surface ($z=0$) than that derived for the Cs atom at $aT3$ ($z=0.49$, corresponding to 2.66 Å above the surface). Suitable reduction of the z parameter for a Cs atom at $T3$ would not only lead to a considerable reduction of the distance to the second-layer Si atom (Si₂) to about 3.3 Å, which might be sterically less favorable, but also to a less favorable orientation of the Cs atom to the Si dangling bonds.

For K/Si(001)(2×1), we determine a comparatively short K_(aD)-Si₍₁₎ distance of 2.90(20) Å which has to be compared with the minimum K-Si bond length of 3.34 Å in

TABLE III. Structure parameters for K/Si(001)(2×1). Lattice constants: $a_0=7.68$ Å, $b_0=3.84$ Å, and $c_0=5.43$ Å. Nonstructural parameters: two scale factors, roughness factor $\beta=0.120(30)$. 135 reflections, unweighted residuum, $R_u=0.089$. Covalent Si-Si distance: 2.35 Å. Theoretical distances: Si-K⁰: 3.53 Å. Si-K⁺: 2.50 Å. Distances in bulk KSi: average distance 3.48 Å (minimum 3.34 Å) [see, e.g., E. Busmann, Z. Anorg. Allg. Chem. **313**, 91 (1961)]. * $B=8\pi^2U$, where U is the mean-squared displacement amplitude.

Atom	x	y	z	ADP (Å ²)	Occupancy
K _(aD)	0.00 ^a	0.20(3)	-0.41(3)	$U^{11}=0.34(15)$ $U^{22}=0.26(15)$ $U^{33}=0.15(5)$	0.25(3)
K _(T3)	0.50 ^a	0.50 ^a	-0.39(2)	$U^{11}=0.45(20)$ $U^{22}=0.09(5)$ $U^{33}=0.40(20)$	0.50(5)
K _(a1T3)	0.34(2)	0.32(4)	-0.51(3)	$B=2.0^{*,a}$	0.10(4)
K _(a2T3)	0.38(3)	0.17(3)	-0.47(3)	$B=2.0^a$	0.10(4)
K _(a1)	0.16(2)	0.23(2)	-0.53(3)	$B=2.0^a$	0.14(4)
Si ₁	0.22(3)	0.00 ^a	0.00 ^a	$U^{11}=0.20(10)$ $U^{22}=0.01^a$ $U^{33}=0.01^a$	1.00 ^a
Si ₂	0.24(3)	0.50 ^a	0.27(2)	$B=3.0^a$	1.00 ^a
Si ₃₁	0.00 ^a	0.50 ^a	0.43(2)	$B=3.0^a$	1.00 ^a
Si ₃₂	0.50 ^a	0.50 ^a	0.42(2)	$B=3.0^a$	1.00 ^a
Si ₄₁	0.00 ^a	0.00 ^a	0.74(2)	$B=3.0^a$	1.00 ^a
Si ₄₂	0.50 ^a	0.00 ^a	0.73(2)	$B=0.9^a$	1.00 ^a
Interatomic distances (Å), error $\approx 0.15-0.30$ Å					
	K _(aD) -Si ₁ :	2.90			
	K _(T3) -Si ₁ :	3.58			
	K _(a1T3) -Si ₁ :	3.17			
	K _(a2T3) -Si ₁ :	2.91			
	K _(a1) -Si ₁ :	3.05			
	K _(T3) -Si ₂ :	4.10			
	Si ₁ -Si ₂ :	2.42			
	Si ₂ -Si ₃₁ :	2.04			
	Si ₂ -Si ₃₂ :	2.16			
	Si ₃₁ -Si ₄₁ :	2.55			
	Si ₃₂ -Si ₄₂ :	2.55			

^aFixed parameter during refinement.

KSi, and 3.30 Å in K₈Si₄₆ [there is also one report of a K_{6,8}Si_{45,3} phase with a minimum K-Si bond length of 3.23 Å (Ref. 34)]. Although this is still well above the K-Si distance which would be obtained assuming a ionic K radius (2.50 Å),⁴⁴ it should be noted in general that due to the large disorder, interatomic distances might be underestimated in the present refinement due to the neglect of anharmonic (non Gaussian) contributions in the ADP's. Keeping this in mind, our results generally indicate shortest A-Si bonds which are at most about 5–10 % shorter than the shortest bonds in the bulk ASi structures. Therefore, our A-Si bond-length determinations are in favor of the picture of a weak polarized covalent A-Si bond.^{21,22} Finally, we comment on the Si-Si bonds in the second and deeper layers. Here we find in general that the Si-Si bond lengths in the first three layers do not deviate more than at most 5–10 % from the bulk Si-Si bond length (2.35 Å). This is comparable with the error bars of the distance determination ($\approx 0.15-0.30$ Å). On the other hand, we determine two distances which are comparatively short,

namely, 2.05 and 2.06 Å (see Tables II and III). However, as in the case of the A's, we observe quite large disorder for the Si atoms as expressed by B factors in the range between 3 and 8 Å² (corresponding to $U=0.04-0.10$ Å²) which might lead to some underestimation (up to about 0.05–0.10 Å) of the interatomic distances. Thus we conclude that the Si-Si bond lengths do not show significant changes as compared to the bulk distance, while the disorder is likely a consequence of the A adsorption induced disorder of the top-layer Si atoms.

(4) The only significant difference between both systems investigated is observed for the total A (saturation) coverage. We determine only about 0.3(1) ML for Cs/Si(001)(2×1) and 1.2(3) ML for K/Si(001)(2×1). Considerable controversy exists about the A saturation coverage in the literature. The double-layer model $P/T3$ (Ref. 10) corresponds to a coverage of 1 ML. This was confirmed by the medium-energy ion scattering study of Ref. 13, which for K and Cs yields a coverage close to 1 ML. However, other

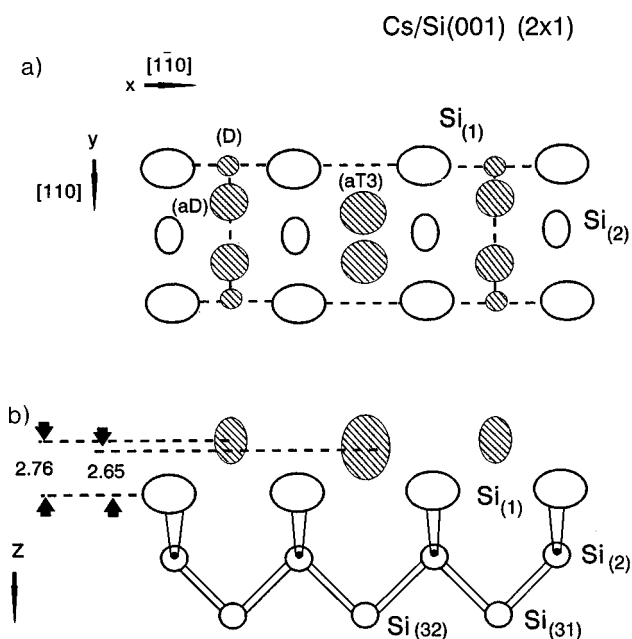


FIG. 3. Schematic drawing of the Cs/Si(001)(2 \times 1) structure in top (a) and side (b) views as derived from the three-dimensional data. Hatched and open circles correspond to Cs and Si atoms, respectively. The relative sizes of the hatched circles are proportional to the Cs occupation factors. The atoms are labeled according to Table II. Significant disorder is emphasized by ellipses such as for Si₍₁₎ (in-plane) as well as for Cs_(aD) and Cs_(aT3) (out of plane).

investigations^{5,26} proposed a saturation coverage of 0.5 ML. Our previous SXRD experiments on Na, K, and Cs on Ge(001)(2 \times 1) (Ref. 7) indicated saturation coverages in the 0.6–0.7 ML regime. From the crystallochemical point of view, a saturation coverage well below 1 ML appears to be reasonable, especially for the larger adsorbate Cs, since a simultaneous full occupancy of two sites within the (2 \times 1)

unit cell (=1 ML) appears not to be possible due to steric reasons. One explanation for the controversy about the saturation coverage might be its critical dependence on the sample preparation. For example, as pointed out by Michel *et al.*⁴⁵ using xenon titration and thermal desorption spectroscopy (TDS), minor changes of the sample temperature around 300 K can lead to dramatic changes in the K coverage on Si(001)(2 \times 1). Further, Soukiassian *et al.*²⁶ showed that trace amounts of surface impurities significantly increase the K-sticking coefficient, which even can lead to A multilayer growth. At last, it should be noted that SXRD only probes the fraction of A's which is adsorbed on definite adsorption sites but is not sensitive to randomly distributed surface adsorbed A. In contrast, it is this integrated amount of adsorbed A which is probed by ion scattering or electron probe techniques.

IV. CONCLUSION

In summary, the SXRD structure analysis of the K/Si(001)(2 \times 1) and the Cs/Si(001)(2 \times 1) surfaces give direct evidence that the A's simultaneously adsorb on different sites on clean Si(001)(2 \times 1). The main adsorption sites are found to be the D site above the dimer rows and the T3 site in the cave between the dimers as well as "asymmetric" sites close to D and T3. The occurrence of multiple adsorption sites is not surprising, since the adsorption is done at room temperature and is not likely to produce an equilibrium structure. The shortest A-Si bond distances are found at most 11% lower than the shortest A-Si bonds in bulk ASi compounds supporting the picture of a weak polarized covalent bond. We have no evidence of a large z disorder of the topmost Si atoms, which would be characteristic of asymmetric dimers. From the average positions of the first layer Si atoms and their large lateral disorder, we conclude that upon A adsorption the Si-Si dimerization is partially lifted.

The adsorption of A's in asymmetric sites has also been found in our previous analysis on the A/Ge(001)(2 \times 1); however, in this case we found A's next to T4, close to the Ge dangling bonds, without breaking the dimerization. This can be interpreted with a weaker interaction between the adsorbed A and the Ge dangling bonds as compared with the A-Si interaction. The driving force for adsorption in these "unusual" sites is suggested to be the formation of a weak covalent bond between the adsorbed A's and the top-layer Si atoms via charge transfer to the dangling bonds, with simultaneous optimization of the bond geometry. Another important result is that for Cs/Si(001)(2 \times 1) the saturation coverage is only about 0.3(1) ML, somewhat lower than 0.5 ML, as suggested by some authors. For K/Si(001) we find 1.2 (3) ML, which within the error bar is still in agreement with the value of 1 ML that is reported by several authors, although this has been critically questioned.

ACKNOWLEDGMENTS

This work was supported by the TMR grant of the European Community. One of us (H.L.M.) would like to acknowledge the hospitality extended to him during his visit in Orsay. The authors also thank R. Wunderlich for the preparation of the figures.

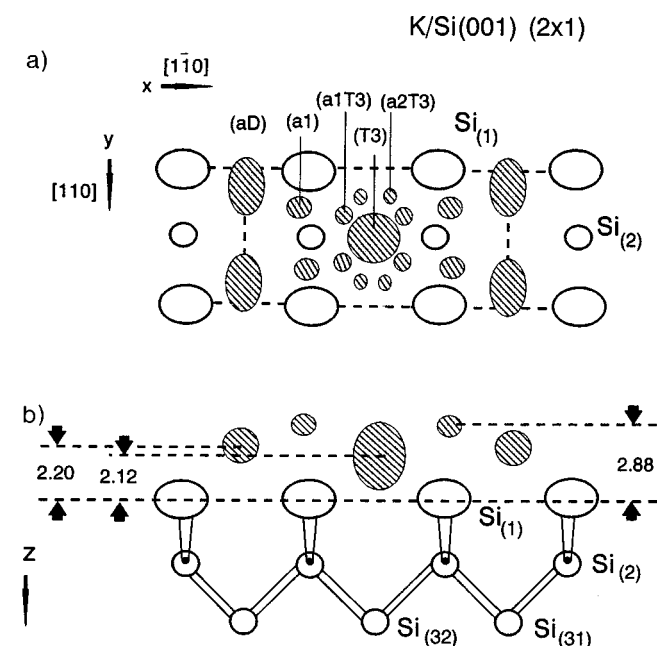


FIG. 4. Schematic view of the K/Si(001)(2 \times 1) structure as in Fig. 3. The atoms are labeled according to Table III.

- ¹ *Metallization and Metal-Semiconductor Interfaces*, Vol. 195 of *NATO Advanced Study Institute, Series B: Physics*, edited by I. P. Batra (Plenum, New York, 1989).
- ² *Physics and Chemistry of Alkali Metal Adsorption*, edited by H. P. Bonzel, A. M. Bradshaw, and G. Ertl (Elsevier, Amsterdam, 1989).
- ³ P. Soukiassian, in *Fundamental Approach to New Materials Phases-Ordering at Surfaces and Interfaces*, edited by A. Yoshimori, T. Shinjo, and H. Watanabe, Springer Series in Materials Science Vol. 17 (Springer-Verlag, Berlin, 1992), p. 197.
- ⁴ E. M. Oellig and R. Miranda, *Surf. Sci.* **177**, L947 (1986).
- ⁵ M. C. Asensio, E. G. Michel, E. M. Oellig, and R. Miranda, *Appl. Phys. Lett.* **51**, 1714 (1987).
- ⁶ We use a sample setting corresponding to a primitive (p) (1×1) surface unit cell which is related to the face (f) centered setting by $[100]_p = 0.5\{[100]_f + [010]_f\}$, $[010]_p = 0.5\{[100]_f - [010]_f\}$, and $[001]_p = [001]_f$. The lattice constants of the (2×1) superstructure unit cell are $a_0 = 3.84 \text{ \AA}$, $b_0 = 7.68 \text{ \AA}$, and $c_0 = 5.43 \text{ \AA}$.
- ⁷ H. L. Meyerheim, R. Sawitzki, and W. Moritz, *Phys. Rev. B* **52**, 16 830 (1995).
- ⁸ J. D. Levine, *Surf. Sci.* **34**, 90 (1973).
- ⁹ Y. Enta, T. Kinoshita, S. Suzuki, and S. Kono, *Phys. Rev. B* **36**, 9801 (1987).
- ¹⁰ T. Abukawa and S. Kono, *Phys. Rev. B* **37**, 9097 (1988).
- ¹¹ S. Tanaka, N. Takagi, N. Minami, and M. Nishijima, *Phys. Rev. B* **42**, 1868 (1990).
- ¹² T. Makita, S. Kohmoto, and A. Ichimiya, *Surf. Sci.* **242**, 65 (1991).
- ¹³ A. J. Smith, W. R. Graham, and E. W. Plummer, *Surf. Sci. Lett.* **243**, L37 (1991).
- ¹⁴ D. Huang and P. R. Antoniewicz, *Phys. Rev. B* **44**, 9076 (1991).
- ¹⁵ Y. Morikawa, K. Kobayashi, K. Terakura, and S. Blügel, *Phys. Rev. B* **44**, 3459 (1991).
- ¹⁶ K. Kobayashi, Y. Morikawa, K. Terakura, and S. Blügel, *Phys. Rev. B* **45**, 3469 (1991).
- ¹⁷ L. S. O. Johansson and B. Reihl, *Phys. Rev. Lett.* **67**, 2191 (1991).
- ¹⁸ T. Urano, Y. Uchida, S. Hongo, and T. Kanaij, *Surf. Sci.* **242**, 39 (1991).
- ¹⁹ T. Urano, S. Hongo, and T. Kanaij, *Surf. Sci.* **287/288**, 294 (1993).
- ²⁰ I. P. Batra, *Phys. Rev. B* **43**, 12 322 (1991).
- ²¹ K. Kobayashi, Y. Morikawa, K. Terakura, and S. Blügel, *Phys. Rev. B* **45**, 3469 (1992).
- ²² P. Küger and J. Pollmann, *Appl. Phys. Lett.* **67**, 2191 (1991).
- ²³ Y.-C. Chao, L. S. O. Johansson, C. J. Karlsson, E. Landemark, and R. I. G. Uhrberg, *Phys. Rev. B* **52**, 2579 (1995).
- ²⁴ Y.-C. Chao, L. S. O. Johansson, and R. I. G. Uhrberg, *Phys. Rev. B* **54**, 5901 (1996).
- ²⁵ Y.-C. Chao, L. S. O. Johansson, and R. I. G. Uhrberg, *Phys. Rev. B* **55**, 7667 (1997).
- ²⁶ P. Soukiassian, J. Kubby, P. Mangat, Z. Hurych, and K. Schirm, *Phys. Rev. B* **46**, 13 471 (1992).
- ²⁷ U. A. Effner, D. Badt, J. Binder, T. Bertrams, A. Brodde, Ch. Lunau, H. Neddermeyer, and M. Hanbücken, *Surf. Sci.* **277**, 207 (1992).
- ²⁸ A. Brodde, Th. Bertrams, and H. Neddermeyer, *Phys. Rev. B* **47**, 4508 (1993).
- ²⁹ R. Feidenhans'l, *Surf. Sci. Rep.* **10**, 105 (1989); I. K. Robinson, in *Handbook of Synchrotron Radiation*, edited by G. S. Brown and D. E. Moncton (Elsevier, Amsterdam, 1991), Vol. III.
- ³⁰ H. L. Meyerheim and R. Sawitzki, *Surf. Sci. Lett.* **301**, L203 (1994).
- ³¹ E. Busmann, *Z. Anorg. Allg. Chem.* **313**, 91 (1961).
- ³² J. Gallmeier, H. Schäfer, and A. Weiß, *Z. Naturforsch. B* **24**, 665 (1969).
- ³³ J. Witte, H. G. Schnering, and W. Klemm, *Z. Anorg. Allg. Chem.* **327**, 260 (1964).
- ³⁴ C. Cros, M. Pouchard, and P. Hagenmüller, *J. Solid State Chem.* **327**, 260 (1970).
- ³⁵ D.-S. Lin, T. Miller, T.-C. Chiang, *Phys. Rev. B* **44**, 10 719 (1991).
- ³⁶ A. Ishizaka, N. Nakagawa, and Y. Shiraki, in *Proceedings of the Second International Symposium on Molecular Beam Epitaxy and Related Clean Surface Techniques* (Japan Society of Applied Physics, Tokyo, 1982).
- ³⁷ The unweighted residuum is defined as: $R_u = \frac{\sum_{hkl} ||F_{hkl}^{obs}|| - |F_{hkl}^{calc}|}{\sum_{hkl} |F_{hkl}^{obs}|}$.
- ³⁸ W. F. Kuhs, *Acta Crystallogr., Sect. A: Found. Crystallogr.* **48**, 80 (1992).
- ³⁹ A. Schmalz, S. Aminpirooz, L. Becker, and L. Haase, *Phys. Rev. Lett.* **67**, 2163 (1991).
- ⁴⁰ R. Fasel, P. Aebi, J. Oserwalder, L. Schlappach, R. G. Agostino, and G. Chiarello, *Phys. Rev. B* **50**, 14 516 (1994).
- ⁴¹ C. Stampfl, J. Neugebauer, and M. Scheffler, *Surf. Rev. Lett.* **1**, 213 (1994).
- ⁴² R. Rossmann, H. L. Meyerheim, V. Jahns, W. Moritz, D. Wolf, D. Dornisch, and H. Schulz, *Surf. Sci.* **279**, 199 (1992).
- ⁴³ C. M. Wei, H. Huang, Y. S. Tong, G. S. Glander, and M. B. Webb, *Phys. Rev. B* **42**, 11 284 (1990).
- ⁴⁴ L. Pauling, *The Nature of the Chemical Bond* (Cornell University Press, Ithaca, NY, 1960).
- ⁴⁵ E. Michel, P. Pervan, G. R. Castro, R. Miranda, and K. Wandelt, *Phys. Rev. B* **45**, 11 811 (1992).